

Protein-Protein Interaction and Conformational Change in the Alpha-Helical Membrane Transporter BtuCD-F in the Native Cellular Envelope

Benesh Joseph^{*[a]}

Alpha-helical membrane proteins perform numerous critical functions essential for the survival of living organisms. Traditionally, these proteins are extracted from membranes using detergent solubilization and reconstitution into liposomes or nanodiscs. However, these processes often obscure the effects of nanoconfinement and the native environment on the structure and conformational heterogeneity of the target protein. We demonstrate that pulsed dipolar electron spin resonance spectroscopy, combined with the Gd^{3+} -nitroxide spin pair, enables the selective observation of the vitamin B_{12} importer BtuCD-F in its native cellular envelope. Despite the

high levels of non-specific labeling in the envelope, this orthogonal approach combined with the long phase-memory time for the Gd^{3+} spin enables the observation of the target protein complex at a few micromolar concentrations with high resolution. In the native envelope, vitamin B_{12} induces a distinct conformational shift at the BtuCD-BtuF interface, which is not observed in the micelles. This approach offers a general strategy for investigating protein-protein and protein-ligand/drug interactions and conformational changes of the alpha-helical membrane proteins in their native envelope context.

Membrane proteins play crucial roles in various cellular processes, making them key targets for drugs.^[1] Traditional methods often rely on purified proteins or reconstitution in artificial lipid environments. However, reconstituted systems may not accurately replicate the complex heterogeneity of the native membranes, and how this affects protein structure and dynamics is often elusive. In recent years, several approaches have been developed to observe outer membrane proteins in their native surroundings.^[2]


Selective observation of α -helical membrane proteins in their native surroundings is still a major challenge for high-resolution techniques such as X-ray crystallography or cryo-EM. On the other hand, spectroscopic observations are challenged by the low expression level and difficulty of selective labeling. Solid-state nuclear magnetic resonance spectroscopy has made significant progress in this direction.^[3] Site-directed spin labeling combined with electron spin resonance (ESR) spectroscopy is a complementary technique for investigating the conformation and heterogeneity of biomolecules, even within their native contexts.^[4] Pulsed ESR spectroscopy techniques, including pulsed electron-electron double resonance (PELDOR or DEER) is ideally suited for such experiments due to their high sensitivity, even at nanomolar concentrations.^[4h,5] Over the past


few years, we demonstrated that PELDOR can be used to observe the outer membrane proteins (OMPs) of *E. coli* in the isolated membranes. In Gram-negative bacteria such as *E. coli*, the cellular envelope consists of an outer membrane (OM) and an inner membrane (IM) separated by the periplasm. Here, the inner membrane was selectively solubilized, which, combined with the natural cysteine-exclusion in OMPs, enabled selective labeling and distance measurements using nitroxide, Gd^{3+} , and trityl labels in the isolated outer membranes.^[6]

However, direct spin labeling and distance determination in the inner membrane (IM) have not yet been demonstrated for α -helical inner membrane proteins (IMPs). Spin-labeled nanobodies were employed to probe IMP conformation in the native envelope.^[4k,l] However, the general application of this approach is severely limited due to the requirement for conformation-specific nanobodies. Unlike the OM, numerous native cysteines of IMPs hinder conventional labeling and PELDOR experiments employing nitroxide labels. In addition to the effect of the native lipids and other interacting partners, the role of nanoconfinement (within the OM-periplasm-IM chamber) on the conformation and interaction of IMPs remains largely unknown.

We reasoned that an orthogonal spin pair would enable us to address the above challenges. In this scenario, the IMP in the envelope can be labeled with a nitroxide label. The specific interaction with an orthogonally labeled (using Gd^{3+} , for example) protein or a ligand and the associated conformational changes can be selectively observed using Gd^{3+} -nitroxide PELDOR. Although this approach has been demonstrated for purified membrane proteins,^[4l,7] extension into the cellular envelope poses several challenges, including the stability of the spin labels, sufficient expression of the IMP, introduction of the interacting partner into the envelope, and detecting the small extent of complex formation in the complex envelope environ-

[a] B. Joseph
Department of Physics, Freie Universität Berlin, Arnimallee 14, Berlin 14195,
Germany
E-mail: benesh.joseph@fu-berlin.de

 Supporting information for this article is available on the WWW under
<https://doi.org/10.1002/cbic.202400858>

 © 2024 The Author(s). ChemBioChem published by Wiley-VCH GmbH. This is
an open access article under the terms of the Creative Commons Attribution
License, which permits use, distribution and reproduction in any medium,
provided the original work is properly cited.

ment. Here, we report a successful application of this approach to observe protein-protein interaction and substrate-induced conformational shift in the ATP-binding cassette (ABC) transporter BtuCD–F.

In *E. coli*, BtuB, which is located in the OM, transports vitamin B₁₂ (VitB₁₂) into the periplasm through the interaction with TonB and the ExbB–ExbD complex.^[8] Subsequently, the periplasmic binding protein BtuF binds and delivers VitB₁₂ to BtuCD, which transports it across the IM at the expense of ATP binding and hydrolysis (Figure 1). The two BtuC subunits, which are inserted into the IM and connected with two solvent-exposed BtuD subunits (which bind and hydrolyze ATP), form an intact ABC transporter.^[9] Structural, biochemical, and biophysical experiments have provided a rather good understanding of the translocation mechanism *in vitro*,^[7a,10] making it an ideal system for further investigations in the native envelope.

We isolated the cellular envelope following overexpression of BtuCD in *E. coli*. A cysteine substitution was introduced on the short loop between the transmembrane helices 5 and 5a (TM5 and TM5a) at T168 in the BtuC subunits (Figure 1 and S1 A). The expression level for BtuCD was optimized by testing various growth conditions, and its presence in the native envelope was further confirmed using western blotting (Figure S1B). Previously, we investigated these positions in micelles, and this variant demonstrated ATPase activity comparable to the wild-type.^[7a,10c] We labeled these cysteines directly in the envelope by incubation with the nitroxide label S-(1-oxyl-2,2,5,5-tetramethyl-2,5-dihydro-1H-pyrrol-3-yl)methyl methanesulfonothioate (MTSL, please see the methods section). The

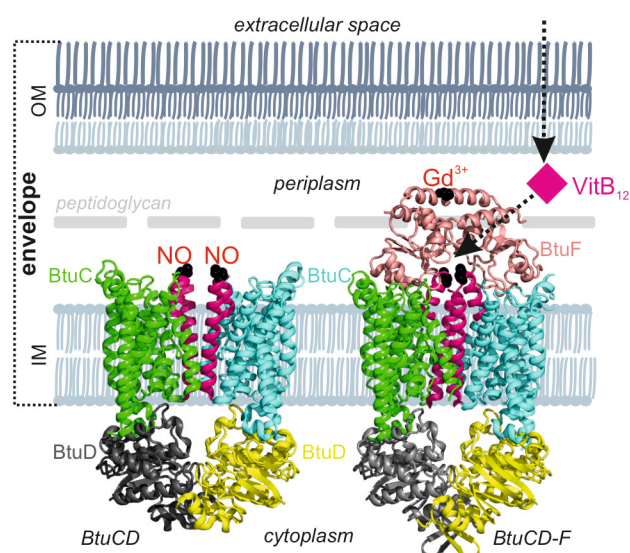


Figure 1. Schematic description of the cell envelope of Gram-negative bacteria. The asymmetric outer membrane (OM), inner membrane (IM), and the periplasm containing a thin peptidoglycan layer are shown. In the periplasm, BtuF binds VitB₁₂ and delivers to BtuCD (on the left in the IM, PDB ID: 1 L7 V) to form the BtuCD–F complex (right, PDB ID: 2QI9), which transports VitB₁₂ into the cytoplasm at the expense of ATP binding and hydrolysis. The spin labeled positions on BtuC (with NO at T168 C) and BtuF (with Gd³⁺ at S138 C) are highlighted as spheres. The TM5–TM5a helices covering the translocation pathway are highlighted in magenta.

MTSL label is stable in the envelope environment for a sufficiently long time (observed up to ~2 h, (Figure S1E).

In the case of the cell envelope, labeling of reactive cysteines in other α -helical proteins will lead to undesired background labeling (Figure S1B–C).^[11] In agreement, we did not observe any difference in the spectral shape and intensity between the cysteine variant and the wild-type protein (Figure S1D). MTSL is stable in the envelope environment (Figure S1E), and the contribution from endogenous Mn²⁺ appears negligible (Figure 2B). Therefore, we adopted an orthogonal labeling strategy by introducing a Gd³⁺ spin label at position S138 C in BtuF (Figure 1 and 2A–B). This BtuF variant efficiently binds to a spin labeled VitB₁₂, thereby revealing a good labeling efficiency (L.E., ~70 %, Figure S2).

The combination of Gd³⁺ with NO provides great advantages, in particular for the envelope sample.^[6,12] By observing BtuF–Gd³⁺ (and pumping NO), distances come exclusively through the interaction with BtuCD, and the effect of non-specific NO labeling is selectively eliminated (which can also be verified with a control sample in which BtuCD is not overexpressed; please see the following sections). Owing to its narrow central transition and favorable relaxation times, Gd³⁺ offers higher sensitivity, especially when combined with the nitroxide spin, which has a narrower spectrum.^[13] Further, this approach provides structural information for BtuF–BtuCD interaction as well as for the TM5–TM5a helices on which the NO labels are located. Relaxation measurements revealed a short phase memory time (T_M , ~800 ns) for the nitroxide-labeled envelope sample (Figure 2C). Remarkably, Gd³⁺–BtuF introduced into the envelope gave a fivefold larger T_M (~4 μ s), thereby facilitating the observation of long dipolar evolution time windows. A NO–NO PELDOR using the envelope gave a broad distribution, which makes it difficult to make any meaningful conclusion (Figure S3A). We also tested another position, D131 C, located away from the membranes on the NBDs, to test whether it is less affected by the non-specific labeling. However, these positions also gave a similarly broad distribution (Figure S3B).

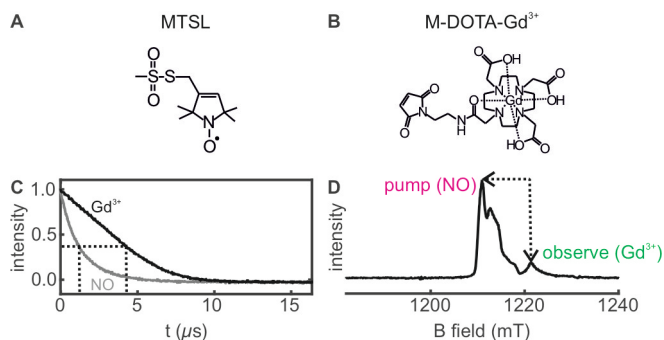


Figure 2. (A, B) Chemical structure of MTSL and maleimide-DOTA–Gd³⁺ labels. (C) Transverse relaxation time measurements for the MTSL labeled *E. coli* envelope, or the Gd³⁺ labeled BtuF introduced into the envelope, in both cases having BtuCD overexpressed. The intensity and the corresponding phase memory times (T_M) are indicated with dotted lines. (D) The echo-detected field-swept spectrum of nitroxide labeled envelope sample containing Gd³⁺ labeled BtuF. The position for the pump (NO) and observer (Gd³⁺) spins are indicated. The measurements were performed at the Q-Band (~34GHz) frequency.

Overall, due to the complexity of the native envelope, a direct distance measurement using cysteine-based labeling, as demonstrated for the outer membrane proteins,^[14] would be difficult.

Notably, the BtuF–Gd³⁺–BtuC–NO PELDOR revealed modulation and interspin distances (Figure 3A–B; please see methods for details of sample preparation). As expected, a similar experiment without BtuCD overexpression did not reveal any distances (Figure S4), thereby confirming that the observed distances arise exclusively from BtuC–BtuF interaction. Another Gd³⁺–Gd³⁺ experiment on this sample gave only an exponential decay, showing that the BtuF molecules are far separated and do not interact within the envelope. The experimental distances are longer than the corresponding simulations (Figure 3B), which might be explained either with a different rotamer distribution or a somewhat increased flexibility at the BtuF–BtuC interface (Figure S5). The rotamer distribution and the distances from the simulation ruled out any steric clashes at these positions in the structure.

The modulation depth (Δ) of the PELDOR data provides quantitative information on the extent of BtuF–BtuC interaction. The Δ is the highest at the point of maximal BtuF–BtuC interaction, and as the fraction of unbound BtuF increases, the Δ will decrease. We observed the maximum Δ (~13%) with 10 μ M BtuF, and it further decreased at higher concentrations,

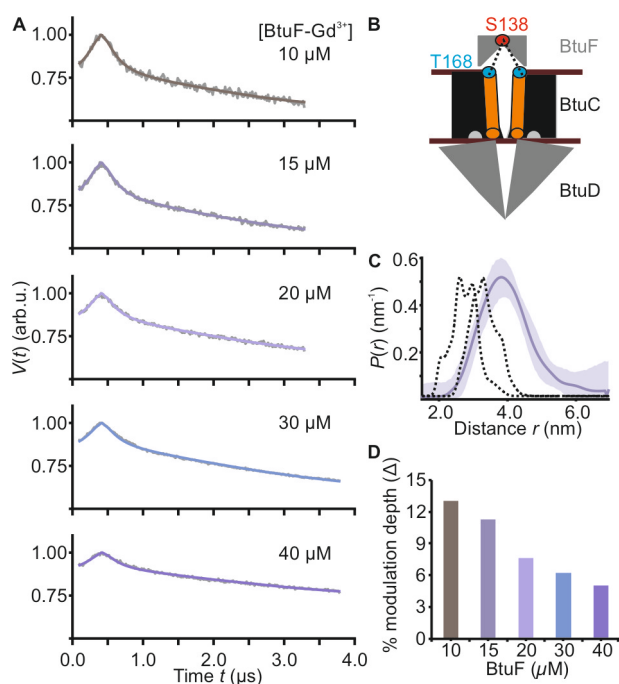


Figure 3. Gd³⁺–BtuF – NO–BtuC PELDOR experiments in the cell envelope of *E. coli*. (A) Data were acquired at increasing concentrations of BtuF–Gd³⁺ added to the MTSL-labeled envelope sample. These data are identical within the S/N. (B) A cartoon for the BtuCD–F structure is shown, highlighting the subunits and the spin labeled positions. The probed distances are indicated with dotted lines. (C) The distance distribution determined using the DeerLab^[15] program for the 15 μ M BtuF sample is presented. Rotamer library-based simulations^[20,21] on the BtuCD–F structure (between BtuF–138 C and the two BtuC–168 C residues, PDB ID: 2QI9) are shown in dotted lines. (D) The observed modulation depths (Δ) at different Gd³⁺–BtuF concentrations are presented.

thereby confirming the specific interaction between BtuF and BtuC (Figure 3A–C). Considering the sub-nanomolar affinity between BtuF and BtuCD,^[9b] this interaction must already be saturated at 10 μ M. With $\Delta_{\text{max}} = \sim 30\%$ under our experimental setup for a two-spin system, it would further increase for a three-spin system (up to $\sim 50\%$) if both BtuF and BtuC are 100% labeled (BtuF has a $\sim 100\%$ L.E., Figure S2). The reduced modulation depth we observed could arise if the amount of BtuC is lower than the added BtuF (10 μ M) and/or due to a lower labeling efficiency for BtuC in the envelope environment (the reality might be a combination of both). Provided that sufficient S/N is achieved, a lower Δ for a multi-spin system helps to eliminate the undesired artifacts.^[16] In summary, the tested conditions allow for reliable PELDOR experiments with BtuCD–F in the native envelope.

Interestingly, the addition of the BtuF+VitB₁₂ complex to BtuCD (called the apo+substrate sample) shifted the distance distribution into a narrower peak centered at ~ 4.5 nm in the envelope (Figure 4A–B) (Figure S6). Notably, this shift is not observed in the detergent-solubilized sample (see blue vs. orange lines in Figure 4B top panel). The data for vanadate-trapped and ADP–Mg²⁺ samples also revealed a similar response. As these distances are nearly the same as for the apo+substrate sample, it can be concluded that the tested nucleotide states do not cause any additional change in the conformation. The presence of VitB₁₂ may alter the MTSL rotamers in the binding pocket (see Figure 1 and inset in Figure 4A). Also, the TM5–TM5a helices carrying the MTSL labels may further move apart to accommodate the VitB₁₂ molecule,

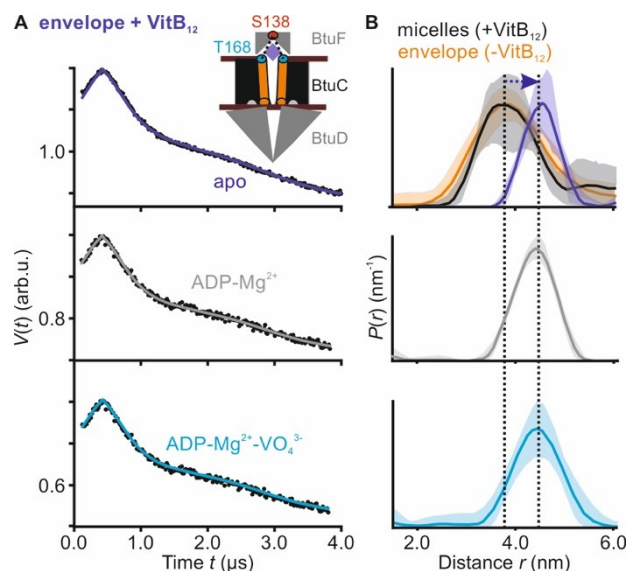


Figure 4. Gd³⁺–BtuF – NO–BtuC PELDOR experiments with VitB₁₂ and/or nucleotides in the cell envelope of *E. coli*. (A) Data were acquired in the presence of BtuF and VitB₁₂ (10 μ M each) in different nucleotide (10 mM each) states as indicated. The cartoon in the inset shows the probed distances. (B) The obtained distance distributions are presented. The distances for the apo state in the absence of VitB₁₂ (in the envelope) are overlaid (orange, taken from Figure 3C) to highlight the shift in the distance distribution, which is further indicated with dotted vertical lines separated by an arrow. The experimental distances for the apo sample in the detergent micelles from our previous study^[7a] are overlaid as well.

and or their overall flexibility can be reduced. (Figure S5). Irrespective of any of these aspects leading to the shift of the distance peak, the data sets suggest that VitB₁₂ must be present inside the BtuCD–F complex. Despite the high data quality, these experiments revealed smaller modulation depth values (5–8%) in comparison to the first set of experiments (Figure 3). As these are biologically independent experiments, we prefer to refrain from a quantitative interpretation of this difference.

In detergent micelles, VitB₁₂ is non-productively released from BtuF upon interaction with BtuCD.^[9c] This is also evident from our data, where VitB₁₂ failed to induce the conformational change in the micelles (Figure 4A, top panel). Thus, no structure for BtuCD–F with bound VitB₁₂ could be yet solved. Therefore, the envelope environment might stabilize the VitB₁₂-bound BtuCD–F complex. A previous study employing radiolabeled VitB₁₂ in proteoliposomes suggested that AMP-PNP (or ATP) is required for trapping VitB₁₂ inside the transporter.^[17] However, subsequent single-molecule fluorescence energy transfer-based studies (in nanodiscs or liposomes) showed that VitB₁₂ could bind to BtuCD–F independent of the nucleotide state,^[10b,d] which is in agreement with our observation of VitB₁₂ inducing the shift in the apo, ADP-Mg²⁺ and the vanadate trapped states (Figure 4). Thus, the release of the P_i following ATP-hydrolysis might be the power stroke for VitB₁₂ translocation.^[7a,9a,d,10b,d]

For spectroscopic investigations in the native membranes, the elimination of the background signals is a major challenge. Here, we overcame this problem with an orthogonal labeling strategy employing Gd³⁺ and NO spin labels combined with protein overexpression. The level of the membrane protein overexpression could be considerably reduced with the ongoing improvements for sensitivity into the nM range.^[5a,b,18] Considering the methodological advances in membrane protein expression, this approach could be successfully applied to any protein or ligand candidate that can be efficiently synthesized and spin-labeled in vitro. This experimental setup is sensitive exclusively to the Gd³⁺–NO spin pairs and thereby detects the specific interaction between the desired molecules. We show that Gd³⁺ labeled BtuF can be introduced into the periplasmic space at sufficient levels. Further, the long T_M for the Gd³⁺ spins enabled the selective and reliable observation of BtuF–BtuCD interaction under the nanoconfinement in the native envelope. This would be a potential tool to elucidate protein–protein or protein–ligand/drug interaction for α -helical membrane protein complexes, including potential antibiotic targets in the native cellular envelope.

Supporting Information Summary

The Supporting Information for protein expression, purification, membrane isolation, spin labeling, and continuous wave and pulsed ESR spectra and analysis are presented. The authors have cited additional references within the Supporting Information.^[19,20]

Acknowledgements

B. J. would like to express sincere gratitude to Sophie Ketter and Jingyi Liu for their support. This work was financially supported through the Emmy Noether program (JO 1428/1-1), SFB 1507 – “Membrane-associated Protein Assemblies, Machineries, and Supercomplexes”, and a large equipment fund (438280639) from the Deutsche Forschungsgemeinschaft to B.J. Open Access funding enabled and organized by Projekt DEAL.

Conflict of Interests

The authors declare no conflict of interest.

Data Availability Statement

The data that support the findings of this study are available from the corresponding author upon reasonable request.

Keywords: Orthogonal spin labeling · In situ structural biology · ABC transporter · DEER or PELDOR · In cell EPR

- [1] A. Galetin, K. L. R. Brouwer, D. Tweedie, K. Yoshida, N. Sjostedt, L. Aleksunes, X. Chu, R. Evers, M. J. Hafey, Y. Lai, P. Matsson, A. Riselli, H. Shen, A. Sparreboom, M. V. S. Varma, J. Yang, X. Yang, S. W. Yee, M. J. Zamek-Gliszczyński, L. Zhang, K. M. Giacomini, *Nat. Rev. Drug Discov.* **2024**, *23*, 255–280.
- [2] a) A. Gopinath, T. Rath, N. Morgner, B. Joseph, *PNAS Nexus* **2024**, *3*, pgae019; b) S. F. Haysom, J. Machin, J. M. Whitehouse, J. E. Horne, K. Fenn, Y. Ma, H. El Mkami, N. Bohringer, T. F. Schaberle, N. A. Ranson, S. E. Radford, C. Pliotas, *Angew. Chem. Int. Ed.* **2023**, *62*, e202218783; c) G. Benn, T. J. Silhavy, C. Kleanthous, B. W. Hoogenboom, *Nat. Comm.* **2023**, *14*, 4772; d) J. Medeiros-Silva, S. Jekhmane, A. L. Paioni, K. Gawarecka, M. Baldus, E. Swiezewska, E. Breukink, M. Weingarth, *Nat. Comm.* **2018**, *9*, 3963; e) B. Joseph, A. Sikora, E. Bordignon, G. Jeschke, D. S. Cafiso, T. F. Prisner, *Angew. Chem. Int. Ed.* **2015**, *54*, 6196–6199.
- [3] a) R. Shukla, F. Lavore, S. Maity, M. G. N. Derks, C. R. Jones, B. J. A. Vermeulen, A. Melcrova, M. A. Morris, L. M. Becker, X. Wang, R. Kumar, J. Medeiros-Silva, R. A. M. van Beekveld, A. Bonvin, J. H. Lorent, M. Lelli, J. S. Nowick, H. D. MacGillavry, A. J. Peoples, A. L. Spoering, L. L. Ling, D. E. Hughes, W. H. Roos, E. Breukink, K. Lewis, M. Weingarth, *Nature* **2022**, *608*, 390–396; b) S. Narasimhan, C. Pinto, A. Lucini Paioni, J. van der Zwan, G. E. Folkers, M. Baldus, *Nat. Protoc.* **2021**, *16*, 893–918; c) H. Xie, Y. Zhao, W. Zhao, Y. Chen, M. Liu, J. Yang, *Sci. Adv.* **2023**, *9*, eadh4168; d) Y. Zhao, H. Xie, L. Wang, Y. Shen, W. Chen, B. Song, Z. Zhang, A. Zheng, Q. Lin, R. Fu, J. Wang, J. Yang, *J. Am. Chem. Soc.* **2018**, *140*, 7885–7895.
- [4] a) B. Joseph, A. Sikora, D. Cafiso, *J. Am. Chem. Soc.* **2016**, *6*, 1844–1847; b) X. Jiang, M. A. Payne, Z. Cao, S. B. Foster, J. B. Feix, S. M. Newton, P. E. Klebba, *Science* **1997**, *276*, 1261–1264; c) S. Jana, E. G. B. Evans, H. S. Jang, S. Zhang, H. Zhang, A. Rajca, S. E. Gordon, W. N. Zagotta, S. Stoll, R. A. Mehl, *J. Am. Chem. Soc.* **2023**, *145*, 14608–14620; d) A. Pierro, M. Drescher, *Chem. Commun.* **2023**, *59*, 1274–1284; e) Y. Shenberger, L. Gevorkyan-Airapetov, M. Hirsch, L. Hofmann, S. Ruthstein, *Chem. Commun.* **2023**, *59*, 10524–10527; f) A. Bonucci, O. Ouari, B. Guigliarelli, V. Belle, E. Mileo, *ChemBiochem* **2020**, *21*, 451–460; g) R. Dastvan, A. Rasouli, S. Dehghani-Ghahnaviyeh, S. Gies, E. Tajkhorshid, *Nat. Comm.* **2022**, *13*, 5161; h) N. Fleck, C. A. Heubach, T. Hett, F. R. Haege, P. P. Bawol, H. Baltruschat, O. Schiemann, *Angew. Chem. Int. Ed.* **2020**, *59*, 9767–9772; i) A. Collauto, S. von Bulow, D. B. Gophane, S. Saha, L. S. Stelzl, G. Hummer, S. T. Sigurdsson, T. F. Prisner, *Angew. Chem. Int. Ed.* **2020**, *59*, 23025–23029; j) S. Maity, B. D. Price, C. B. Wilson, A. Mukherjee, M. Starck, D. Parker, M. Z. Wilson, J. E. Lovett, S. Han, M. S. Sherwin, *Angew. Chem. Int. Ed.* **2023**, *62*, e202212832; k) L. Galazzo, G. Meier, D.

- Janulienė, K. Parey, D. De Vecchis, B. Striednig, H. Hilbi, L. V. Schafer, I. Kuprov, A. Moeller, E. Bordignon, M. A. Seeger, *Sci. Adv.* **2022**, *8*, eabn6845; l) L. Galazzo, G. Meier, M. H. Timachi, C. A. J. Hutter, M. A. Seeger, E. Bordignon, *Proc. Natl. Acad. Sci. U. S. A.* **2020**, *117*, 2441–2448; m) C. Cheng, R. F. Tsai, C. K. Lin, K. T. Tan, V. Kalendra, M. Simenas, C. W. Lin, Y. W. Chiang, *JACS Au* **2024**, *4*, 3766–3770.
- [5] a) K. Ackermann, C. A. Heubach, O. Schiemann, B. E. Bode, *J. Phys. Chem. Lett.* **2024**, *15*, 1455–1461; b) S. Kucher, C. Elsner, M. Safonova, S. Maffini, E. Bordignon, *J. Phys. Chem. Lett.* **2021**, *12*, 3679–3684; c) Y. Ben-Ishay, Y. Barak, A. Feintuch, O. Ouari, A. Pierro, E. Mileo, X. C. Su, D. Goldfarb, *Protein Sci.* **2024**, *33*, e4903; d) T. F. Cunningham, M. R. Putterman, A. Desai, W. S. Horne, S. Saxena, *Angew. Chem. Int. Ed.* **2015**, *54*, 6330–6334; e) K. Ackermann, S. Khazaipoul, J. L. Wort, A. I. S. Sobczak, H. E. Mkami, A. J. Stewart, B. E. Bode, *J. Am. Chem. Soc.* **2023**, *145*, 8064–8072; f) N. Hoang, E. Schleicher, S. Kacprzak, J. P. Bouly, M. Picot, W. Wu, A. Berndt, E. Wolf, R. Bittl, M. Ahmad, *PLoS Biol.* **2008**, *6*, e160; g) A. Pierro, A. Bonucci, A. Magalon, V. Belle, E. Mileo, *Chem. Rev.* **2024**, *124*, 9873–9898; h) M. Rudolph, R. Tampe, B. Joseph, *Angew. Chem. Int. Ed.* **2023**, e202307091.
- [6] S. Ketter, B. Joseph, *J. Am. Chem. Soc.* **2023**, *145*, 960–966.
- [7] a) B. Joseph, V. M. Korkhov, M. Yulikov, G. Jeschke, E. Bordignon, *J. Biol. Chem.* **2014**, *289*, 3176–3185; b) M. D. Sophie Ketter, Olga Rogozhnikova, Sergey A. Dobrynin, Victor M. Tormyshev, Elena G. Bagryanskaya, Benesh Joseph, *J. Mag. Reson. Open* **2022**, *10-11*, 100041.
- [8] H. Celia, I. Botos, X. Ni, T. Fox, N. De Val, R. Lloubes, J. Jiang, S. K. Buchanan, *Commun. Biol.* **2019**, *2*, 358.
- [9] a) V. M. Korkhov, S. A. Mireku, D. B. Veprintsev, K. P. Locher, *Nat. Struct. Mol. Biol.* **2014**, *21*, 1097–1099; b) O. Lewinson, A. T. Lee, K. P. Locher, D. C. Rees, *Nat. Struct. Mol. Biol.* **2010**, *17*, 332–338; c) R. N. Hvorup, B. A. Goetz, M. Niederer, K. Hollenstein, E. Perozo, K. P. Locher, *Science* **2007**, *317*, 1387–1390; d) K. P. Locher, A. T. Lee, D. C. Rees, *Science* **2002**, *296*, 1091–1098.
- [10] a) M. Priess, H. Goddeke, G. Groenhof, L. V. Schafer, *ACS Cent. Sci.* **2018**, *4*, 1334–1343; b) M. Yang, N. Livnat Levanon, B. Acar, B. Aykac Fas, G. Masrati, J. Rose, N. Ben-Tal, T. Haliloglu, Y. Zhao, O. Lewinson, *Nat. Chem. Biol.* **2018**, *14*, 715–722; c) B. Joseph, G. Jeschke, B. A. Goetz, K. P. Locher, E. Bordignon, *J. Biol. Chem.* **2011**, *286*, 41008–41017; d) J. M. H. Goudsmits, D. J. Slotboom, A. M. van Oijen, *Nat. Commun.* **2017**, *8*, 1652.
- [11] B. Joseph, A. Sikora, E. Bordignon, G. Jeschke, D. S. Cafiso, T. F. Prisner, *Angew. Chem. Int. Ed.* **2015**, *54*, 6196–6199.
- [12] L. Galazzo, M. Teucher, E. Bordignon, *Methods Enzymol.* **2022**, *666*, 79–119.
- [13] a) I. Kaminker, H. Yagi, T. Huber, A. Feintuch, G. Otting, D. Goldfarb, *Phys. Chem. Chem. Phys.* **2012**, *14*, 4355–4358; b) P. Lueders, G. Jeschke, M. Yulikov, *J. Phys. Chem. Lett.* **2011**, *2*, 604–609.
- [14] B. Joseph, E. A. Jaumann, A. Sikora, K. Barth, T. F. Prisner, D. S. Cafiso, *Nat. Protoc.* **2019**, *14*, 2344–2369.
- [15] L. Fabregas Ibanez, G. Jeschke, S. Stoll, *Magn. Reson. (Gott)* **2020**, *1*, 209–224.
- [16] a) K. Ackermann, B. E. Bode, *Mol. Phys.* **2018**, *116*, 1513–1521; b) T. von Hagens, Y. Polyhach, M. Sajid, A. Godt, G. Jeschke, *Phys. Chem. Chem. Phys.* **2013**, *15*, 5854–5866.
- [17] V. M. Korkhov, S. A. Mireku, K. P. Locher, *Nature* **2012**, *490*, 367–372.
- [18] J. L. Wort, K. Ackermann, A. Giannoulis, A. J. Stewart, D. G. Norman, B. E. Bode, *Angew. Chem. Int. Ed.* **2019**, *58*, 11681–11685.
- [19] a) M. Teucher, E. Bordignon, *J. Mag. Reson.* **2018**, *296*, 103–111; b) C. E. Tait, S. Stoll, *Phys. Chem. Chem. Phys.* **2016**, *18*, 18470–18485.
- [20] Y. Polyhach, E. Bordignon, G. Jeschke, *Phys. Chem. Chem. Phys.* **2011**, *13*, 2356–2366.
- [21] G. Jeschke, *Protein Sci.* **2021**, *30*, 125–135.

Manuscript received: October 17, 2024

Revised manuscript received: November 16, 2024

Accepted manuscript online: November 17, 2024

Version of record online: November 28, 2024